



ORIGINAL ARTICLE

White tea extract modified green synthesis of magnetite supported Ag nanoparticles: Evaluation of its catalytic activity, antioxidant and anti-colon cancer effects



De-Zhi Hou^a, Ping Ling^a, Yu Zhu^a, Yi-Ming Ouyang^{a,*1}, Bikash Karmakar^b

^a Department of General Surgery I, The First People's Hospital of Yunnan Province. The Affiliated Hospital of Kunming University of Science and Technology, Kunming, Yunnan, China.

^b Department of Chemistry, Gobardanga Hindu College, 24 Parganas (North), India

Received 30 May 2022; accepted 26 August 2022

Available online 31 August 2022

KEYWORDS

Silver;
Magnetic;
White tea extract;
Pyrano[3,2-*c*]chromene;
Colon cancer;
Antioxidant

Abstract In this study, an eco-friendly and low-cost procedure for the synthesis of *White tea* plant extract modified magnetic nanocomposite ($\text{Fe}_3\text{O}_4@W.tea$) has been demonstrated. Ag nanoparticles (Ag NPs) were further decorated *in situ* over the designed $\text{Fe}_3\text{O}_4@W.tea$ nanocomposite exploiting the plant derived phytochemicals as bio-reductant and stabilizer. The resulting $\text{Fe}_3\text{O}_4@W.tea/\text{Ag}$ nanocomposite was characterized by various analytical methods like Fourier Transformed Infra Red (FT-IR) spectroscopy, scanning electron microscopy (SEM), energy-dispersive X-ray spectroscopy (EDS), energy dispersive X-ray analysis (EDX) elemental mapping, transmission electron microscopy (TEM), vibrating-sample magnetometer (VSM), X-ray diffraction analysis (XRD), and inductively coupled plasma-atomic emission spectrometry (ICP-AES) analysis. The as-synthesized bio-nanomaterial was used as an excellent heterogeneous and magnetically retrievable catalyst in the three-component condensation of 4-hydroxycoumarin, malononitrile and various aldehydes in refluxing aqueous media. A broad range of aromatic aldehydes underwent the reaction to produce diverse pyrano[3,2-*c*]chromene derivatives in very good yields irrespective of the nature of bearing functional groups or their respective geometrical positions. Due to superparamagnetic character, the material was easily magnetically decanted out and recycled for 8 successive times with preservation of its catalytic activity. After the chemical applications we also explored the material biologically in the resistance of human colon cancer and thereby studied the cytotoxicity over two

* Corresponding author.

E-mail address: oyym1625@sina.com (Y.-M. Ouyang).

¹ ORCID ID: 0000-0002-5698-0867.

Peer review under responsibility of King Saud University.



standard cell lines, HT-29 and Caco-2. The conventional MTT assay was carried out over them which revealed an increase in % cell viability dose dependently. The IC_{50} values observed in the two cell lines were 384.2 $\mu\text{g/ml}$ and 254.6 $\mu\text{g/ml}$ respectively. In addition, DPPH radical scavenging test was performed for studying anti-oxidant activity. The results validate the administration of $\text{Fe}_3\text{O}_4@W.tea/\text{Ag}$ nanocomposite as a competent colon protective drug in the clinical trial studies over human.

© 2022 Published by Elsevier B.V. on behalf of King Saud University. This is an open access article under the CC BY-NC-ND license (<http://creativecommons.org/licenses/by-nc-nd/4.0/>).

1. Introduction

Throughout the last decade, silver nanoparticles (Ag NPs) have garnered significant attention all over the world in the realm of applied material research due to its unique features like considerable chemical stability, localized surface plasmon resonance, high catalytic activity and outstanding conductivity (Galdiero et al., 2011; Siddiqi et al., 2018; Sharma et al., 2009; Singh et al., 2015; Calderón-Jiménez et al., 2017). They display plethora of implications in multidimensional domains like medicinal therapeutics, agriculture, material sciences, bio-sensing, optics, plasmonics, electronics etc (Islam et al., 2021; Aziz et al., 2015; Baghayeri et al., 2018a,b; Mirfakhraei et al., 2018; Veisi et al., 2019; Maleki et al., 2014; Maleki et al., 2010; Hamelian et al., 2018a,b; Veisi et al., 2016; Veisi, 2011; Veisi et al., 2021; Baghayeri, et al., 2018; He et al., 2021; Zomorodian et al., 2018; Hemmati et al., 2020). According to earlier reports Ag NPs are able to generate reactive oxygen species (ROS) around their surface that has significant biological advantages, particularly in displaying antifungal or antimicrobial activities (Dakal et al., 2016; Kim et al., 2011; Burdusel et al., 2018; Akhavan, 2009). It also shows significant wound healing properties in the form of topical administration (Burdusel et al., 2018). Another important biological activity displayed by Ag NPs is their anti-tumor and anti-cancer properties (Chinnasamy et al., 2021; Aziz et al., 2019; Karimi Ghezeli et al., 2019). Some general methods for the preparation of Ag NPs include the chemical, photochemical and sonochemical reduction, application of microwave irradiation, microemulsions and some hybrid methods (Oves et al., 2018; Irvani et al., 2014). Although some of these procedures are very effective and practical, the involvement of toxic, harsh and unsafe chemicals, high temperature in the liquid or gaseous environment, high energy protocols, irksome methods for purification, prolonged synthesis and expensiveness restrain their practical use in bulk scale or industrial domains (Nadagouda et al., 2011). In the recent times green and biogenic method of synthesis of NPs have come up with enormous eminence, which basically involve different organisms like bacteria, fungi, algae and plant extract following a sustainable and biocompatible pathway (Kowshik et al., 2003; Ahmed et al., 2016; Zhang et al., 2016).

Nevertheless, the use of plant extract as the green and natural resource for biotemplating the synthesis of NPs has been more beneficial due to several reasons. In this procedure there is minimal chance of chemical or microbial contamination which is highly detrimental in diverse medicinal applications (Jouyandeh et al., 2022). This method is absolutely green and energy efficient as it involves water as reaction media and the procedure is maintained at ambient conditions (Mohanpuria et al., 2008; Rai and Ingle, 2012). The polar phyto-molecules contained therein create a liophilic environment that enables the sustainable reduction of incoming metal ions into corresponding NPs. The as-synthesized NPs are also produced in uniform dimension with very unique homogeneous distribution. Furthermore, these biogenic metal NPs are remarkably stable due to capping by the biomolecules (Akhtar et al., 2013; Durán et al., 2011; Ballotin et al., 2016; Azmath et al., 2016; Cai et al., 2022). Extract of different parts of the plant (leaves, flower, fruit, seed, root, bark, gum etc) have been used in the biogenic synthesis these green nanomaterials. Several recent reports have been encountered for the biogenic Ag NPs using leaves

extract of *Citrus limon* (Vankar and Shukla, 2012); *Murraya koenigii* (Philip et al., 2011); *Nelumbo nucifera* (Santhoshkumar et al., 2011); *Hibiscus cannabinus* (Bindhu and Umadevi, 2013); flower extract of *Thymbra spicata* (Veisi et al., 2018); *Tagetes erecta* (Katta and Dubey, 2021); *Catharanthus roseus* (Kandiah and Chandrasekharan, 2021); fruit extract of *Embelica officinalis* (Ankamwar et al., 2005); *Phyllanthus embelica* (Masum et al., 2019), seed extract of *Bunium persicum* (Vartooni et al., 2016), *Tectona grandis* (Rautela et al., 2019); root extract of *Morinda citrifolia* (Suman et al., 2013); *Duchesnea indica* (Ilahi et al., 2021), green tea extract of *Camellia sinensis* (Nakhjavani et al., 2017), latex of *Jatropha gossypifolia* (Borase et al., 2014) etc.

In this connection, we would like to report the use of white tea extract in the bio-inspired synthesis of green Ag NPs, being supported over magnetic Fe_3O_4 NPs. In the stepwise synthesis, Ag NPs were bio-synthesized *in situ* over the magnetic NPs. White tea is a naturally occurring tea plant that is prepared from the first leaves of *Camellia sinensis* species and being minimally processed. This facilitates it to have rich concentration in biomolecules like non-protein amino acids, catechins, epicatechin, gallic acid, gallic acid gallate, epicatechin gallate and alkaloids as compared to green or black tea (Prashanth et al., 2019; David et al., 2021; Haghparasti and Shahri, 2018). As the tiny Ag NPs have high tendency to self-aggregate, the Fe_3O_4 NPs have been preferred as effective support that would promote the uniform dispersion of Ag NPs over them and keep them away from each other. Moreover, the magnetic core would also help to retrieve the composite material from the application pot (Shahriari et al., 2021).

Finally, after the synthesis, the $\text{Fe}_3\text{O}_4@W.tea/\text{Ag}$ nanocomposite material was explored as a heterogeneous reusable nanocatalyst in the one-pot multicomponent synthesis of diverse pyrano[3,2-c]chromene derivatives. Among the biologically imperative oxygenated heterocycles chromene derivatives, more explicitly, the pyranochromenes engross momentous concentration. The scaffold has been found to construct the spine of an array of naturally occurring biomolecules and drugs. In addition, they demonstrate a wide spectrum of molecular activities like antibacterial, antiviral, antitumor, anticancer, antihypertensive, anticoagulant, anti-HIV, anti-infertility, antidepressant, anti rheumatic and several others (Gourdeau et al., 2004; Chetan et al., 2012; Burgard et al., 1999; Evans et al., 1984; Zhang et al., 2016; Mungra et al., 2011; Bonsignore et al., 1993; Saundane et al., 2013; Makawana et al., 2012; Venkatesham et al., 2012; Jagadishbabu and Shivashankar, 2017; Shivashankar et al., 2006; Shivashankar et al., 2007; Maleki et al., 2019; Maleki et al., 2019; Maleki et al., 2017; Maleki et al., 2017). Despite the variety of competent catalytic methodologies reported in the synthesis of pyrano[3,2-c]chromene derivatives (Ghashang et al., 2014; Ghashang et al., 2015; Baziar and Ghashang, 2016; Ghashang, 2016; Ghashang, 2016; Ghashang et al., 2016; Ghashang et al., 2016; Singh et al., 2012; Pradhan et al., 2014; Wang et al., 2010; Vala et al., 2016; Mansoor et al., 2015; Brahmachari and Banerjee, 2014), there always remains abundant scopes for its further development. In this protocol we have followed clean and absolutely green pathway with several advantages like excellent productivity in short time, isolation of products by simple filtration and subsequent recrystallization evading chromatographic techniques, facile magnetic retrieval of catalyst with several times reusability etc.

Furthermore, we evaluated the biological activity of $\text{Fe}_3\text{O}_4@W.tea/Ag$ nanocomposite in controlling the growth of colorectal carcinoma in human body. Cytotoxicity of the material was determined over two standard colorectal cell lines HT-29 and Caco-2 following standard MTT assay. Colorectal cancer (CRC) is one of the most lethal and invasive cancer which attacks human gastrointestinal system and causes high mortality (Dong et al., 2019; Lin et al., 2020). The conventional treatment procedures like chemotherapy, immunotherapy, targeted therapy, hormonal therapy, radiotherapy and surgery have been recorded to involve several recurrent side effects like damage of nerves, toxicity, hair loss, fatigue, diarrhea, swelling or bruising of the incision area etc (Han et al., 2019; Valeri, 2019). In search of the unconventional drug formulations noble metal NPs have acquired significant attention in furnishing excellent anticancer effects without any adversity (Abdel-Fattah and Ali, 2018; Patil and Kim, 2017; Bisht and Rayamajhi, 2016; Hassanien et al., 2018). It has been a very recent trend to indulge different bio-engineered or biogenic noble metal NPs in the high-end cancer research. In our research also we achieve some excellent results against the colorectal carcinoma cell lines in addition to very good antioxidant properties.

2. Experimental:

2.1. Preparation of white tea extract

2.0 g of dried white tea leaves were washed thoroughly with deionized water and warmed in 50 mL deionized water upto 80°C for 30 min. It was filtered through Whatman-1 filter paper and the pale yellow colored filtrate was used as the white tea extract.

2.2. Green synthesis of the $\text{Fe}_3\text{O}_4@W.tea/Ag$ nanocomposite

Fe_3O_4 NPs were synthesized according to the literature following co-precipitation method (Hamelian et al., 2018a,b; Veisi et al., 2016; Veisi, 2011; Veisi et al., 2021; Baghayeri, et al., 2018). 0.5 g of the dried and activated NPs were dispersed in 50 mL deionized water by sonication for 20 min. Subsequently, 20 mg AgNO_3 was added to the mixture and stirred for 30 min in order to immobilize the Ag ions over Fe_3O_4 support. The white tea extract was then introduced as the green reductant and stabilizer of the tiny Ag NPs. The $\text{Fe}_3\text{O}_4@W.tea/Ag$ nanocomposite was finally isolated using a bar magnet, washed with deionized water and dried at 60°C .

2.3. General procedure for the synthesis of pyrano[3,2-c]chromene derivatives

A mixture of 4-hydroxycoumarin (1 mmol), aromatic aldehyde (1 mmol), and malononitrile (1 mmol) and $\text{Fe}_3\text{O}_4@W.tea/Ag$ catalyst (25 mg) was refluxed in water (5 mL) for an appropriate time. After completion (by TLC), the catalyst was removed by external magnet and the precipitated crude product was filtered. It was further purified by recrystallization from hot EtOH. All the products were known and therefore we just confirmed their melting points and authenticated with standard.

2.4. Antioxidant analysis

In antioxidant investigation of $\text{Fe}_3\text{O}_4@W.tea/Ag$ nanomaterial, the well-known 1,1-diphenyl-2-picrylhydrazil (DPPH)

radical scavenging assay was followed. By principle, the purple colored DPPH radical methanolic solution was brought in contact to the probe sample when the radical is quenched by abstracting protons or free electrons from the antioxidant material and assumes a yellow color. The antioxidant capacity of the sample is proportional to the intensity of yellow color of resulting solution, as measured spectrophotometrically.

2.5. Cytotoxic activity

Cytotoxicity of the $\text{Fe}_3\text{O}_4@W.tea/Ag$ nanomaterial was measured over the HT-29 and Caco-2 colorectal cell lines following standard MTT assay. At the outset the cell lines were cultured in 1×10^5 cell/well in 96-well plates inside a humidified incubator at usual conditions (37°C , 5 % CO_2 atmosphere) for 24 h. When the cell confluence was about 80–85 % in a monolayer, the media (10 % FBS) was decanted off and the cells were washed twice with PBS. The experimental nanomaterial was prepared in five different concentrations (0.5, 5, 50, 500, and 1000 $\mu\text{g}/\text{mL}$) in RPMI medium and introduced into the processed cells. The mixtures were incubated again for 72 h under the same conditions followed by the addition of 10 μL solution of MTT dye in PBS (5 mg/mL). They were put into the incubator once again for 4 h. The cell media was likewise replaced with 100 μL DMSO and shaken to facilitate the formazan crystal solubilization. Finally, absorbance of the color complexes were determined at 545 nm equipped with a ELISA microplate reader.

3. Results and discussion

3.1. Characterization and data analysis of $\text{Fe}_3\text{O}_4@W.tea/Ag$ nanocomposite

In this research we have demonstrated a sustainable procedure for the synthesis of biogenic Ag NPs over magnetic Fe_3O_4 NPs using White tea extract as green reducing and stabilizing agent ($\text{Fe}_3\text{O}_4@W.tea/Ag$ nanocomposite). The stepwise synthesis involved the plant biomolecules functionalization over Fe_3O_4 -NPs which is followed by immobilization of Ag^+ ions and subsequent green reduction of the ions into NPs *in situ* (Scheme 1). After successful synthesis, the nanocomposite particles were retrieved easily using a magnet. ICP-OES analysis revealed the Ag load on the material being 0.13 mmol g^{-1} . The structural, morphological and physicochemical properties of $\text{Fe}_3\text{O}_4@W.tea/Ag$ nanocomposite were determined by different analytical techniques like FT-IR, SEM, EDX, TEM, ICP-OES, VSM and XRD study.

Fig. 1 embodies the comparative FT-IR spectra of unmodified Fe_3O_4 NPs, pure white tea extract and $\text{Fe}_3\text{O}_4@W.tea/Ag$ nanocomposite. Fe_3O_4 NP (Fig. 1a) is recognized by the specific peaks observed at 445 and 583 cm^{-1} , ascribed to the octahedral bending and tetrahedral stretching vibrations of Fe—O—Fe bond. The spinel arrangement was verified from the peak found at observed at 631 cm^{-1} . O—H stretching vibrations due to hydroxyl groups present over the ferrite surface and O—H bending vibrations due to adsorbed water molecules were characterized by the two vibrational bands detected at 3420 and 1635 cm^{-1} respectively. Conversely, the corresponding peaks due to the phytochemicals present in the white tea extract has been displayed in Fig. 1b. The organic biomolecu-



Scheme 1 Schematic green synthesis of Fe₃O₄@W.tea/Ag nanocomposite mediated by *White tea* extract and its applications for synthesis of pyrano[3,2-*c*]chromene derivatives.

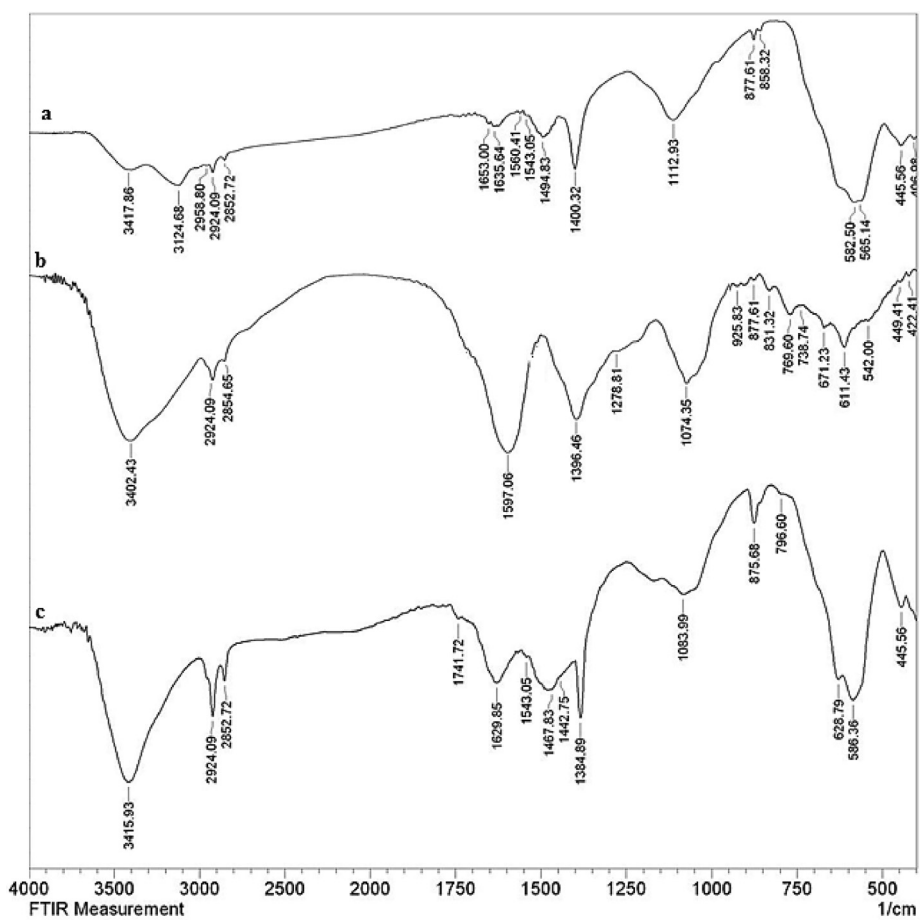


Fig. 1 The FT-IR spectra of Fe₃O₄NPs (a), *White tea* extract (b) and green synthesized Fe₃O₄@W.tea/Ag nanocomposite (C).

lar functions were detected by the array of bond vibrations found at 3402, 2924, 1597, 1396 and 1074 cm^{-1} , being related to O—H stretching, C—H stretching, C=C stretching, C—O stretching and C—O—C stretching vibrations respectively, validating the occurrence of polyols, flavanols, tannins, catechins, alkaloids and terpenoids in the tea extract. Fig. 1c displays the FT-IR characteristics of $\text{Fe}_3\text{O}_4@W.tea/\text{Ag}$ nanocomposite, which is very similar to a hybrid of Fig. 1a and b. The slight shift in the individual bond vibrations in Fig. 1c can be personified, due to the strong coordination of Ag NPs with the bio-functions and surface hydroxyl groups.

Electron microscopic analysis (TEM and SEM) were performed in order to have a knowledge on the surface morphology, texture, particle distribution, particle size and shape of $\text{Fe}_3\text{O}_4@W.tea/\text{Ag}$ nanocomposite (Figs. 2 and 3). TEM image shows (Fig. 2) a clear distribution of the two different kind of nanoparticles, both within the range of 15–20 nm dimension. The grey and black colored particles represents Fe_3O_4 and Ag NP respectively. By shape, both the particles are uniformly spherical and well apart from each other. No significant particle agglomeration is detected from the image. The shade like manifestation is believed to be due to surface anchoring by white tea phytochemicals over Fe_3O_4 NPs. The advantage of having high surface area of the ferrite NPs was exploited in anchoring of plant phytochemicals which was further used in the green reduction of the incoming metal ions and subsequently reducing them to corresponding NPs. They were additionally stabilized by the plant biomolecules. SEM image also confirms the globular shaped NPs, although looks somewhat aggregated due to sample preparation manually (Fig. 3). However, the two kind of NPs as well as the plant functionalization are not detectable separately from SEM.

After having the surface morphological information we carried out the EDX analysis, equipped with the SEM instrument, in order to know its chemical composition. As Fig. 4 displays, $\text{Fe}_3\text{O}_4@W.tea/\text{Ag}$ nanocomposite is composed of Fe and Ag as metal and C, O as non metals. A major peak of Au is found at 2.1 keV, attributed to the sample coating by Au vapor deposition. The non-metals in the profile correspond to the phyto-molecular association. The EDX results were furthermore emphasized by elemental mapping. X-ray scanning of a section of the SEM image results the dispersion pattern of the constituent elements (Fig. 5). Markedly, the elemental species in the form of dots are quite uniformly distributed over the surface. The uniform distribution definitely has superior effect on its catalytic activity.

The crystalline structure and phase behavior of the $\text{Fe}_3\text{O}_4@W.tea/\text{Ag}$ nanocomposite was resolved by XRD analysis and the corresponding profile has been depicted in Fig. 6. The appearance of sharp diffraction peaks validates the material to be of high crystallinity. Analysis of the signals observed $2\theta = 30.7, 36.1, 44.2, 54.5, 58.1, 63.6^\circ$ justify their matching with JCPDS standard 19-0629, related to diffraction on (220), (311), (400), (422), (511) and (440) Fe_3O_4 crystal planes. However, the additional peaks observed at $2\theta = 39.6^\circ, 45.3^\circ, 68.5^\circ$ and 77.9° belong to the diffraction on (111), (200), (220) and (311) planes of Ag face-centred cubic (fcc) crystals (JCPDS No. 87-720). The poorly crystalline broad hump within the 20° diffraction angle is the characteristic of tea extract biomolecular attachment.

Based on the iron core, the study of magnetic properties of $\text{Fe}_3\text{O}_4@W.tea/\text{Ag}$ nanocomposite is an ubiquitous task.

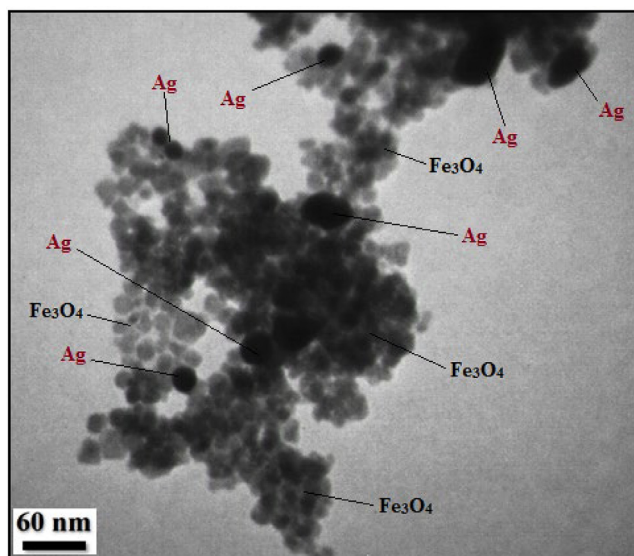


Fig. 2 TEM image of $\text{Fe}_3\text{O}_4@W.tea/\text{Ag}$ nanocomposite.

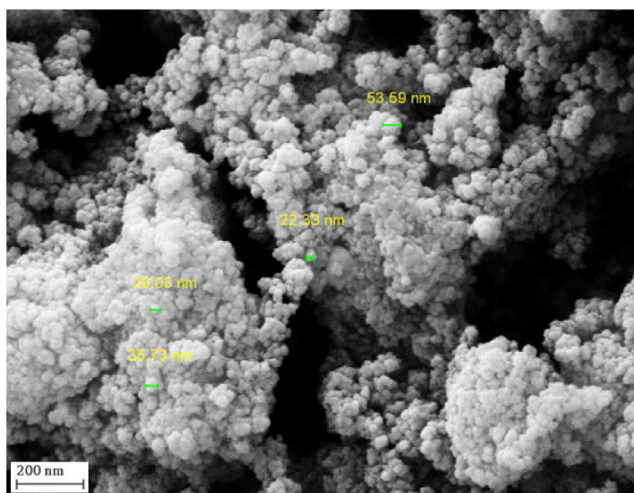


Fig. 3 SEM image of $\text{Fe}_3\text{O}_4@W.tea/\text{Ag}$ nanocomposite.

Thereby, VSM analysis was performed over it and the corresponding profile is shown in Fig. 7. It displays a magnetic hysteresis curve, with a magnetization saturation (M_s) value of 52.8 emu/g, indicating the material to be of superparamagnetic in nature and easy magnetically retrievable.

3.2. The catalytic application of $\text{Fe}_3\text{O}_4@W.tea/\text{Ag}$ nanocomposite in the synthesis of pyrano[3,2-c]chromenes

After the detailed characterizations of the $\text{Fe}_3\text{O}_4@W.tea/\text{Ag}$ nanocomposite, we surveyed the material as catalyst in the three component condensation of 4-hydroxycoumarin, malono nitrile and variety of aryl aldehyde towards the synthesis of 2-amino-4-aryl-4,5-dihydropyrano[3,2-c]chromene-3-carbonitrile derivatives (Scheme 1). At the outset, standardization of reaction conditions were appeared very important and thereby different parameters like the nature of solvent, amount of catalyst and temperature were employed on a probe reac-

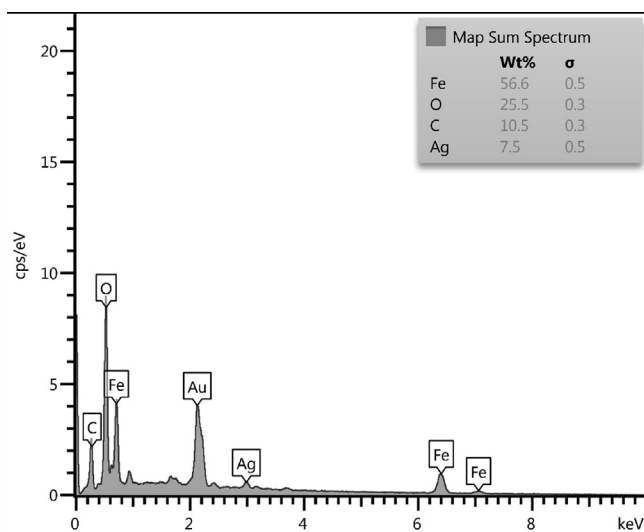


Fig. 4 EDX spectrum of $\text{Fe}_3\text{O}_4@W.tea/Ag$ nanocomposite.

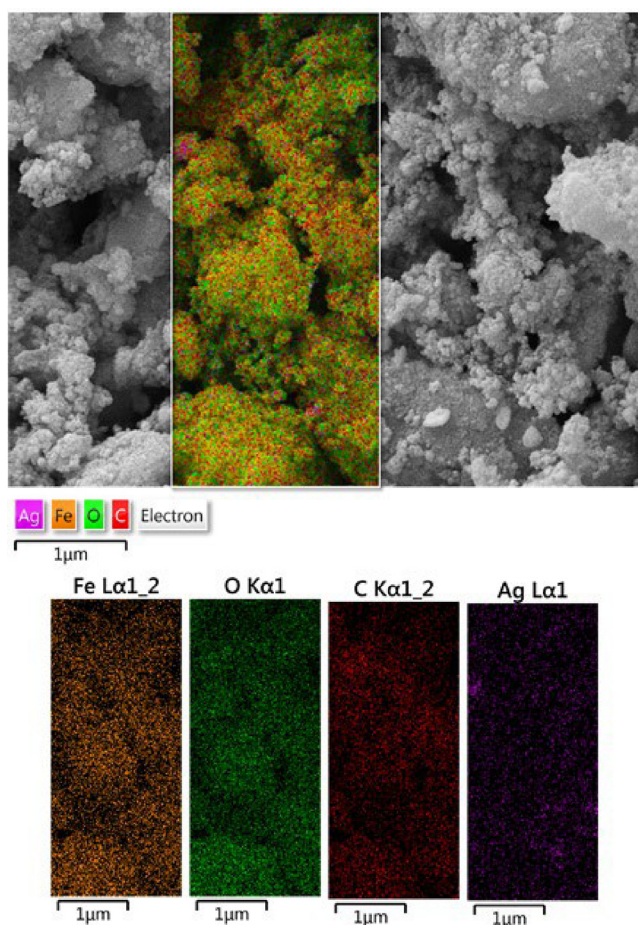


Fig. 5 SEM image of $\text{Fe}_3\text{O}_4@W.tea/Ag$ nanocomposite with its elemental mapping.

tion using benzaldehyde along with the other reagents in presence of $\text{Fe}_3\text{O}_4@W.tea/Ag$ catalyst (Table 1). In the screening of this reaction using diverse solvents like EtOH, hexane, $\text{CH}_3\text{-Cl}$, CH_2Cl_2 , toluene, acetonitrile and water (entries 1–7) at

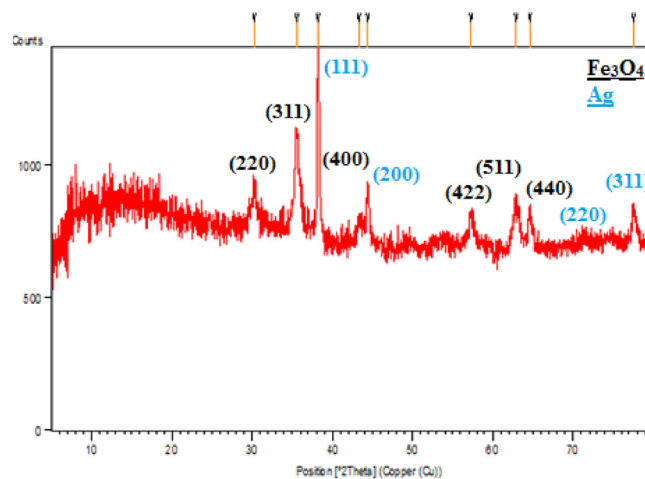


Fig. 6 XRD pattern of $\text{Fe}_3\text{O}_4@W.tea/Ag$ nanocomposite.

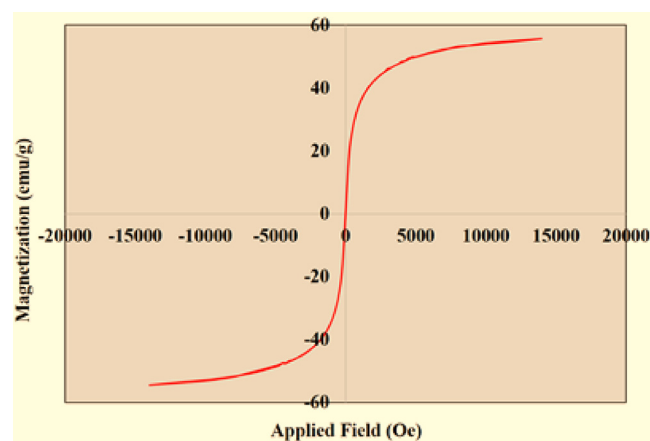
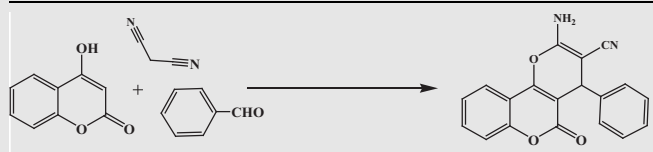


Fig. 7 VSM analysis of $\text{Fe}_3\text{O}_4@W.tea/Ag$ nanocomposite.

their respective reflux temperatures, the best result was obtained in water affording 96 % yields in just 2 h (Entry 7). Next, we opted for the variation of catalyst amount keeping the best solvent and 25 mg was observed to be the optimum (entries 7–9). Even on application a higher catalyst load (30 mg), there was no further improvement in the yield (entry 8). Noticeably, there was only a trace of product under catalyst free condition even after heating the reagents in water which proves the active role of the catalyst (entry 11). Again, the reaction was not very successful at room temperature even under the best solvent and catalytic conditions (entry 10). So, we had the best condition with equimolar reagents under refluxing water (5 mL) in presence of 25 mg of $\text{Fe}_3\text{O}_4@W.tea/Ag$ nanocatalyst.

Subsequently, we moved forward to test the scope and generality of those optimized conditions by variation of substrates and thereby employed a range of aromatic and heteroaromatic aldehydes carrying variable functionalities to react with 4-hydroxycoumarin and malononitrile. The results are demonstrated in Table 2. Irrespective of the electronic effect of functional groups, being electron donating (Me, OMe, NMe_2 , OH) or withdrawing (NO_2 , Cl, Br), all the substrates were very

Table 1 Optimization of the reaction conditions for the synthesis of pyrano[3,2-*c*]chromene derivatives over $\text{Fe}_3\text{O}_4@W.tea/Ag$ nanocatalyst.^a


Entry	Solvent	Catalyst (mg)	Temp.	Time (h)	Yield (%)
1	EtOH	25	80 °C	3	75
2	hexane	25	70 °C	5	30
3	CH ₃ Cl	25	60 °C	5	40
4	CH ₂ Cl ₂	25	40 °C	5	45
5	Toluene	25	110 °C	3	60
6	CH ₃ CN	25	82 °C	4	75
7	H₂O	25	100 °C	2	96
8	H ₂ O	30	100 °C	2	96
9	H ₂ O	20	100 °C	3	90
10	H ₂ O	25	25 °C	10	45
11	H ₂ O	0	100 °C	10	15

^a Reaction conditions: 4-hydroxycoumarin (1 mmol), aldehydes (1 mmol), malononitrile (1 mmol), and solvent (5 mL) in the presence of $\text{Fe}_3\text{O}_4@W.tea/Ag$ catalyst.

Table 2 $\text{Fe}_3\text{O}_4@W.tea/Ag$ catalyzed synthesis of pyrano[3,2-*c*]chromene derivatives.^a

Entry	Aldehyde	Time (h)	Yield (%) ^b	Mp (°C)	Mp (°C) ^{ref}
1	C ₆ H ₅ CHO	2	96	256–258	255–257 (Baziar and Ghashang, 2016)
2	4-Me-C ₆ H ₄ CHO	3	90	256–258	255–257 (Baziar and Ghashang, 2016)
3	4-MeO-C ₆ H ₄ CHO	5	96	249–251	248–250 (Baziar and Ghashang, 2016)
4	3-NO ₂ -C ₆ H ₄ CHO	3	90	263–265	262–264 (Baziar and Ghashang, 2016)
5	4-Cl-C ₆ H ₄ CHO	2	96	258–260	259–261 (Baziar and Ghashang, 2016)
6	2-Cl-C ₆ H ₄ CHO	3	90	274–276	274–276 (Baziar and Ghashang, 2016)
7	4-N(Me) ₂ -C ₆ H ₄ CHO	5	88	225–227	225–227 (Baziar and Ghashang, 2016)
8	2-Br-C ₆ H ₄ CHO	3	80	293–295	294–296 (Pradhan et al., 2014)
9	2,4-Cl ₂ -C ₆ H ₃ CHO	3	95	260–262	260–262 (Baziar and Ghashang, 2016)
10	4-OH-C ₆ H ₄ CHO	5	80	274–276	265–267 (Baziar and Ghashang, 2016)
11	3-OH-C ₆ H ₄ CHO	6	80	269–271	268–270 (Baziar and Ghashang, 2016)
12	2-furylaldehyde	5	80	251–253	251–253 (Baziar and Ghashang, 2016)

^a General procedure: 4-hydroxycoumarin (1 mmol), aldehydes (1 mmol), malononitrile (1.0 mmol), $\text{Fe}_3\text{O}_4@W.tea/Ag$ (25 mg), H₂O (5 mL) at 100 °C.

^b Yield of isolated product.

much compatible producing excellent yields (entries 1–11). There was no marked effect on the geometry of functional groups too.

3.3. Study of reaction mechanism and reusability

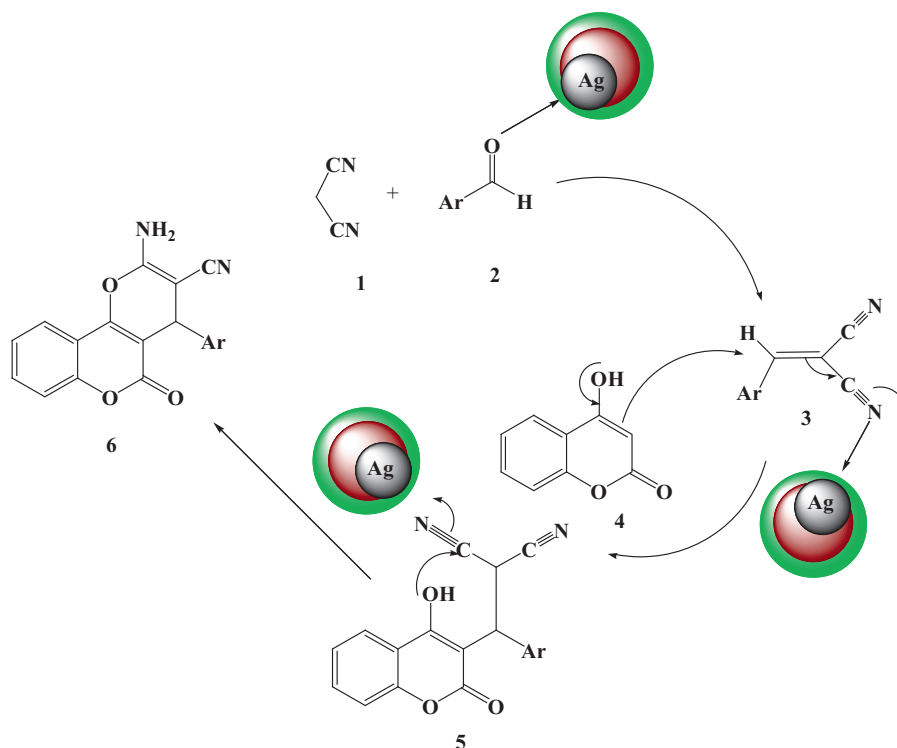
While concerning about the reaction pathway, this is proposed that malononitrile (1) initially reacts with the activated aromatic aldehyde (2) following Knoevenagel condensation to produce the Michael acceptor intermediate 3. In the mean time, 4-hydroxy coumarin (4), undergoes Michael addition with the this activated intermediate. The Michael adduct (5) as synthesized, involves itself into an internal cyclocondensation leading to the final product 2-amino-4-aryl-4,5-dihydro

pyrano[3,2-*c*]chromene-3-carbonitrile(6), leaving the catalyst site free for further use (Scheme 2).

As the catalyst involves magnetic core inside, that was retrieved from the reaction mixture quite easily using a magnet. It was washed with aqueous ethanol and dried for regeneration. The material was robust enough to be reused for a rigorous 8 times recycling in succession without considerable decrease in its activity (Fig. 8).

3.4. Study of antioxidant potential of $\text{Fe}_3\text{O}_4@W.tea/Ag$ nanocomposite

Several earlier *in vitro* analysis suggested the excellent antioxidant activity of Ag nanomaterials, either in pristine or com-



Scheme 2 Proposed mechanism for the synthesis of 2-amino-4-aryl-4,5-dihydropyrano[3,2-c]chromene-3-carbonitrile.

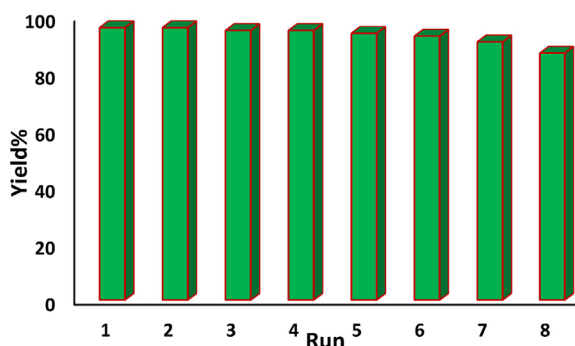


Fig. 8 The reusability of $\text{Fe}_3\text{O}_4@W.tea/Ag$ nanocomposite.

posite form. They were observed to scavenged the DPPH radical with significant potential, indicating the promising use of Ag nanocomposites as practical antioxidants for maintenance of health against different oxidative stress related to degenerative diseases. Due to the enhanced surface to volume ratio, these nanomaterials have large number of free active electrons available on their surface which facilitates to scavenge the free radicals, thereby increasing the antioxidant potential. They also ameliorate the generation of oxidants, the reactive oxygen species (ROS), decrease the oxidative damages and increase the antioxidant defense system in the body (Amani et al., 2017). In addition, the white tea extract contains certain polyphenols that individually are very good antioxidants (Wang et al., 2019). Again, there are reports which says the antioxidant

capacity of polyphenols gets enhanced in presence of iron oxides due to their excellent redox properties (Akhavan et al., 2012). Obviously, the combination of these three components would have much superior antioxidant properties. Accordingly, the $\text{Fe}_3\text{O}_4@W.tea/Ag$ nanomaterial was explored in the DPPH assay *in vitro*. In our protocol, sample solutions were prepared in different concentrations (31.25, 62.5, 125, 250, 500 and 1000 $\mu\text{g}/\text{mL}$) and mixed to equal volume of DPPH solution in methanol (150 μL , 0.04 mg/mL). Each of the mixtures were incubated at 37 $^\circ\text{C}$ for 30 min in dark and finally UV absorbance of the resulting solutions were estimated spectrophotometrically at 517 nm. The following equation was used to calculate the antioxidant potential in terms of % inhibition.

$$\text{Inhibition (\%)} = \left(1 - \frac{\text{Abs}_{\text{sample}} - \text{Abs}_{\text{blank}}}{\text{Abs}_{\text{control}} - \text{Abs}_{\text{blank}}}\right) \times 100$$

Abs sample: absorbance of the reaction mixture, *Abs blank*: absorbance of the blank for each sample dilution in DPPH solvent, *Abs control*: absorbance of DPPH solution in sample solvent.

Fig. 9 displays the output observed in the said investigation which reveals the % inhibition capacity of the nanocomposite material increases dose-dependently and becomes the maximum at a concentration of 1000 $\mu\text{g}/\text{mL}$ (90.25 %).

3.5. Cytotoxicity studies over $\text{Fe}_3\text{O}_4@W.tea/Ag$ nanocomposite

Nanomaterials exhibiting high antioxidant potential are reported to display excellent cytotoxicity and anticancer activity. Several articles have been reported to explain this

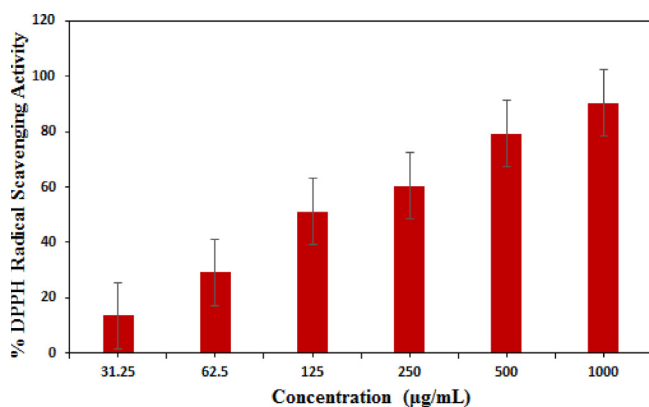


Fig. 9 Antioxidant activity of $\text{Fe}_3\text{O}_4@W.tea/Ag$ nanocomposite.

bioactivity shown by the nanomaterials. In presence of light the nanomaterials may generate active superoxide radicals or radical anions which further induces different reactive oxygen species (ROS). These ROS actively take part in destroying or at least intervene the growth the cancer cells. The ROS have the ability to trap the cancer cells and disconnect them from their growth media resulting inhibit their proliferation. Another mechanism is reported to involve the direct contact interaction of very sharp edges of nanomaterial to the cell walls of the targeted cells and thereafter damaging the cell DNA. In addition, the polyphenols are observed to have high tendency to attach over cancer cells as compared to normal cells (Dutta et al., 2015; Akhavan et al., 2011; Akhavan et al., 2012; Abdolahad et al., 2013). In the determination of cytotoxicity following MTT assay, the HT-29 and caco-2 colorectal cell lines were cultured in standard manner and brought in contact to the Ag nanocomposite material. The polyphenol functionalized Ag NPs use to reduce the ATP content of the cell strongly which causes the damage of mitochondria. This in turn, increases the generation of reactive oxygen species of Ag ions thereby enhancing its cytotoxic activity. In our protocol the $\text{Fe}_3\text{O}_4@W.tea/Ag$ nanocomposites was prepared in five different concentrations (5–2000 µg/mL) and after the cell treatments MTT solution was added to each of them. The optical density of formazan product was evaluated to determine the % cell viability according to the given equation.

$$\text{Toxicity}\% = \left(1 - \frac{\text{mean OD of sample}}{\text{mean OD of control}}\right) \times 100$$

$$\text{Viability}\% = 100 - \text{Toxicity}\%$$

Figs. 10 and 11 depicts the % toxicity of cells treated with various concentration of the nanocomposite. Evidently, they increases with increasing dose of the samples. The corresponding IC_{50} values were determined as 384.2 µg/ml and 254.6 µg/ml. This investigation evidently tells the significant antiproliferative effect of $\text{Fe}_3\text{O}_4@W.tea/Ag$ nanocomposites. Nevertheless, this could be due to the synergetic influence of Ag NPs and white tea bioactive phytochemicals functionalized over the surface matrix. Still, additional detailed studies are required to comprehend the underneath mechanism behind the excellent anticancer activity of our devised material.

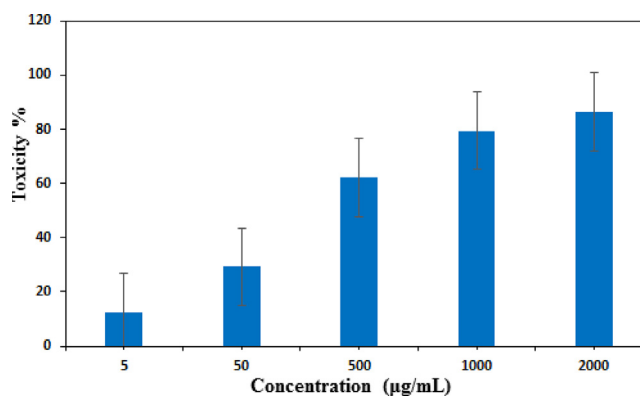


Fig. 10 *In vitro* toxicity analysis of $\text{Fe}_3\text{O}_4@W.tea/Ag$ nanocomposite on HT-29 cell.

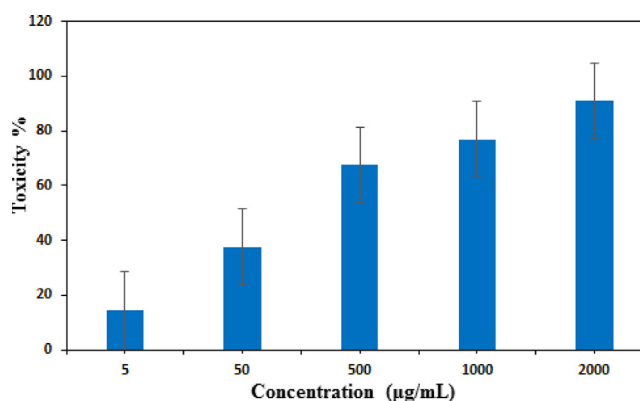


Fig. 11 *In vitro* toxicity analysis of $\text{Fe}_3\text{O}_4@W.tea/Ag$ nanocomposite on Caco-2 cell.

4. Conclusion

In summary, we have demonstrated herein, a sustainable green approach towards the fabrication and synthesis of tiny Ag NPs decorated Fe_3O_4 NPs using white tea extract as a green reducing and stabilizing agent, avoiding the use of any harmful reducing or capping agents. The biotemplated synthesis facilitates to produce uniformly spherical shaped Ag NPs being homogeneously dispersed over the magnetite support. The as synthesized material features were affirmed by several physicochemical analyses. TEM study displayed the material dimension in the range of just 15–20 nm which affords large surface area and various unique catalytically and biologically viable properties. XRD study also justified the material to be of very good crystallinity. Heading towards the catalytic application, the $\text{Fe}_3\text{O}_4@W.tea/Ag$ nanocomposite material showed outstanding activity in the multicomponent synthesis of 2-amino-4-aryl-4,5-dihydroprano[3,2-c]chromene-3-carbonitrile derivatives by combining 4-hydroxycoumarin, malonitrile and diverse aromatic aldehydes producing very good yields. In addition, the material was explored as an chemotherapeutic nanomedicine with non-conventional formulation against the human colorectal cancer. HT-29 and Caco-2 cell lines were used in the determination of cytotoxicity following traditional MTT assay which showed the increasing % toxicity dose dependently. In addition, the material was found to display very good antioxidant potential, as validated through DPPH radical scavenging assay. So, we believe these very activities exhibited by the $\text{Fe}_3\text{O}_4@W.tea/Ag$

Agnanocomposite material would definitely drag attention of scientific communities for using in industrial arena and biomedical sector in larger scale.

Declaration of Competing Interest

The authors declare that they have no known competing financial interests or personal relationships that could have appeared to influence the work reported in this paper.

Acknowledgement

B. Karmakar thanks Gobardanga Hindu College for providing research facilities and technical supports.

References

- Abdel-Fattah, W.I., Ali, G.W., 2018. *J. Appl. Biotechnol. Bioeng.* 5 (2), 00116.
- Abdolahad, M., Janmaleki, M., Mohajerzadeh, S., Akhavan, O., Abbasi, S., 2013. *Mater. Sci. Eng., C* 33, 1498–1505.
- Ahmed, S., Ahmad, M., Swami, B.L., Ikram, S., 2016. *J. Adv. Res.* 7, 17–28.
- Akhavan, O., 2009. *J. Colloid Interface Sci.* 336, 117–124.
- Akhavan, O., Ghaderi, E., Esfandiari, A., 2011. *J. Phys. Chem. B* 115 (2011), 6279–6288.
- Akhavan, O., Kalaei, M., Alavi, Z.S., Ghiasi, S.M.A., Esfandiari, A., 2012. *Carbon* 50, 3015–3025.
- Akhavan, O., Ghaderi, E., Akhavan, A., 2012. *Biomaterials* 33, 8017–8025.
- Akhtar, M.S., Panwar, J., Sun, Y.S., 2013. *ACS Sustainable Chem. Eng.* 6, 591–602.
- Amani, H., Habibey, R., Hajmiresmail, S., Latifi, S., Pazoki-Toroudi, H., Akhavan, O., 2017. *J. Mater. Chem. B* 5, 9452–9476.
- Ankamwar, B., Damle, C., Ahmad, A., Sastry, M., 2005. *J. Nanosci. Nanotechnol.* 5, 1665–1671.
- Aziz, N., Faraz, M., Pandey, R., Shakir, M., Fatma, T., Varma, A., et al., 2015. *Langmuir* 31, 11605–11612.
- Aziz, N., Sherwani, A., Faraz, M., Fatma, T., Prasad, R., 2019. *Front. Chem.* 7, 65.
- Azmah, P., Baker, S., Rakshith, D., Satish, S., 2016. *Saudi Pharm. J.* 24, 140–146.
- Baghayeri, M., Veisi, H., Farhadi, S., Beitollahi, H.I., Maleki, B., 2018a. *J. Iran. Chem. Soc.* 15 (5), 1015–1022.
- Baghayeri, M., Ansari, R., Nodehi, M., Veisi, H., 2018b. *Int. J. Environ. Anal. Chem.* 98, 874–888.
- Ballotin, D., Fulaz, S., Souza, M.L., Corio, P., Rodrigues, A.G., Souza, A.O., et al., 2016. *Nanoscale Res. Lett.* 11, 313.
- Baziar, A., Ghashang, M., 2016. *React. Kinet. Mech. Catal.* 118, 463–479.
- Bindhu, M.R., Umadevi, M., 2013. *Spectrochim. Acta Part A Mol. Biomol. Spectrosc.* 101, 184–190.
- Bisht, G., Rayamajhi, S., 2016. *Nanobiomedicine* 3, 1.
- Bonsignore, L., Loy, G., Secci, D., Calignano, A., 1993. *Eur. J. Med. Chem.* 28, 517–520.
- Borase, H.P., Patil, C.D., Salunkhe, R.B., Suryawanshi, R.K., Salunkhe, B.K., Patil, S.V., 2014. *Bioprocess Biosyst. Eng.* 37, 1695–1717.
- Brahmachari, G., Banerjee, B., 2014. *ACS Sustainable Chem. Eng.* 2, 411.
- Burdusel, A.C., Gherasim, O., Grumezescu, A.M., Mogoantă, L., Ficai, A., Andronescu, E., 2018. *Nanomater.* 8, E681.
- Burgard, A., Lang, H.J., Gerlach, U., 1999. *Tetrahedron* 55, 7555–7562.
- Cai, Y., Karmakar, B., Alsalem, H.S., El-kott, A.F., Bani-Fwaz, M. Z., et al., 2022. *Arab. J. Chem.* 15, 103848.
- Calderón-Jiménez, B., Johnson, M.E., Montoro Bustos, A.R., Murphy, K.E., Winchester, M.R., Vega Baudrit, J.R., 2017. *Front. Chem.* 5 (6), 1–26.
- Chetan, B.S., Nimesh, M.S., Manish, P.P., Ranjan, G.P., 2012. *J. Serb. Chem. Soc.* 77, 1–17.
- Chinnasamy, G., Chandraekharan, S., Koh, T.W., Bhatnagar, S., 2021. *Front. Microbiol.* 12, 611560.
- Dakal, T.C., Kumar, A., Majumdar, R.S., Yadav, V., 2016. *Front. Microbiol.* 16, 1831.
- David, S.R., Abdullah, K., Shanmugam, R., Thangavelu, L., Das, S. K., Rajabalaya, R., 2021. *BioNanoScience* 11, 1095–1107.
- Dong, J., Li, J., Luo, J., Wu, W., 2019. *Eur. J. Inflammation* 17, 1.
- Durán, N., Marcato, P.D., Durán, M., Yadav, A., Gade, A., Rai, M., 2011. *Appl. Microbiol. Biotechnol.* 90, 1609–1624.
- Dutta, T., Sarkar, R., Pakhira, B., Ghosh, S., Sarkar, R., et al., 2015. *RSC Adv.* 5, 80192–80195.
- Evans, J.M., Fake, C.S., Hamilton, T.C., Poyser, R.H., Showell, G. A., 1984. *J. Med. Chem.* 27, 1127–1131.
- Galdiero, S., Falanga, A., Vitiello, M., Cantisani, M., Marra, V., Galdiero, M., 2011. *Molecules* 16, 8894–8918.
- Ghashang, M., 2016. *Res. Chem. Intermed.* 42, 4191–4205.
- Ghashang, M., 2016. *Biointerface Res. Appl. Chem.* 6, 1338–1344.
- Ghashang, M., Mansoor, S.S., Aswin, K., 2014. *Chin. J. Catal.* 35, 127–133.
- Ghashang, M., Kargar, M., Shafiee, M.R.M., Mansoor, S.S., Fazlinia, A., Esfandiari, H., 2015. *Recent Pat. Nanotech.* 9, 204–211.
- Ghashang, M., Mansoor, S.S., Shams Solaree, L., Sharifian-Esfahani, A., 2016. *Iran. J. Catal.* 6, 237–243.
- Ghashang, M., Mansoor, S.S., Mohammad Shafiee, M.R., Kargar, M., NajafiBiregan, M., Azimi, F., Taghrir, H., 2016. *J. Sulfur Chem.* 37, 377–390.
- Gourdeau, H., Leblond, L., Hamelin, B., Desputeau, C., Dong, K., Kianicka, I., Custeau, D., Boudreau, C., Geerts, L., Cai, S.-X., et al., 2004. *Mol. Cancer Ther.* 3, 1375–1384.
- Haghparsati, Z., Shahri, M.M., 2018. *Mater. Sci. Eng., C* 87, 139–148.
- Hamelian, M., Hemmati, S., Varmira, K., Veisi, H., 2018a. *J. Taiwan Inst. Chem. Eng.* 93, 21–30.
- Hamelian, M., Varmira, K., Veisi, H.J., 2018b. *Photochem. Photobiol. B Biol.* 184, 71–79.
- Han, Y.D., Oh, T.J., Chung, T.H., 2019. *Clinical Epigenetics* 11, 51.
- Hassanien, R., Husein, D.Z., Al-Hakkani, M.F., 2018. *Heliyon* 12, e01077.
- He, C., Guo, Y., Karmakar, B., El-kott, A., Ahmed, A.E., Khames, A., 2021. *J. Environ. Chem. Eng.* 9.
- Veisi, Hemmati, H., Shirvani, S., Veisi, H., 2016. *Appl. Organomet. Chem.* 30, 387–391.
- Hemmati, S., Heravi, M.M., Karmakar, B., Veisi, H., 2020. *J. Mol. Liq.* 319, 114302.
- Ilahi, I., Khuda, F., Sahibzada, M.U.K., Alghamdi, S., Ullah, R., et al., 2021. *Arab J Chem.* 14, 103110.
- Iravani, S., Korbekandi, H., Mirmohammadi, S.V., Zolfaghari, B., 2014. *Res. Pharm. Sci.* 9, 385–406.
- Islam, M.A., Jacob, M.V., Antunes, E., 2021. *J. Environ. Manage.* 281, 111918.
- Jagadishbabu, N., Shivashankar, K., 2017. *J. Heterocyclic Chem.* 54, 1543–1549.
- Jouyandeh, M., Tavakoli, O., Sarkhanpour, R., Sajadi, S.M., Zarrintaj, P., et al., 2022. *J. Hazard. Mater.* 424, 127294.
- Kandiah, M., Chandrasekharan, K.N., 2021. *J. Nanotechnol.* 5512786.
- Karimi Ghezeli, Z., Hekmati, M., Veisi, H., 2019. *Appl. Organomet. Chem.* 33.
- Veisi, H., 2011. *Curr. Org. Chem.* 15, 2438–2468.
- Veisi, H., Karmakar, B., Tamoradi, T., Hemmati, S., Hekmati, M., Hamelian, M., 2021. *Sci. Rep.* 11, 1–13.

- Katta, V.K.M., Dubey, R.S., 2021. *Mater. Today Proceed.* 45, 794–798.
- Kim, S.H., Lee, H.S., Ryu, D.S., Choi, S.J., Lee, D.S., 2011. *Korean J. Microbiol. Biotechnol.* 39, 77–85.
- Kowshik, M., Ashtaputre, S., Kharrazi, S., Vogel, W., Urban, J., Kulkarni, S.K., et al., 2003. *Nanotechnology* 14, 95.
- Lin, A., Zhang, J., Luo, P., 2020. *Front. Immunol.* 11, 2039.
- Makawana, J.A., Patel, M.P., Patel, R.G., 2012. *ArchivDerPharmazie* 345, 314–322.
- Maleki, B., Azarifar, D., Veisi, H., Hojati, S.F., Salehabadi, H., Yami, R.N., 2010. *Chin. Chem. Lett.* 21, 1346–1349.
- Maleki, B., Hemmati, S., Sedrpoushan, A., Ashrafi, S.S., Veisi, H., 2014. *RSC Adv.* 4 (76), 40505–40510.
- Maleki, A., Jafari, A.A., Yousefi, S., 2017. *Carbohydr. Polym.* 175, 409–416.
- Maleki, A., Movahed, H., Ravaghi, P., 2017. *Carbohydr. Polym.* 156, 259–267.
- Maleki, A., Niksefat, M., Rahimi, J., Ledari, R.-T., 2019. *Mater. Today Chem.* 13, 110–120.
- Maleki, A., Varzi, Z., Afruzi, F.-H., 2019. *Polyhedron* 171, 193–202.
- Mansoor, S.S., Logaiya, K., Aswin, K., Sudhan, P.N., 2015. *J. Taibah Univ. Sci.* 9, 213–226.
- Masum, M.M.I., Siddiqa, M.M., Ali, K.A., Zhang, Y., Abdallah, Y., Ibrahim, E., Qiu, W., Yan, C., Li, B., 2019. *Front. Microbiol.* 10, 820.
- Mirfakhraei, S., Hekmati, M., Eshbala, F.H., Veisi, H., 2018. *New J. Chem.* 42, 1757–1761.
- Mohanpuria, P., Rana, N.K., Yadav, S.K., 2008. *J. Nanopart. Res.* 10, 507–517.
- Mungra, D.C., Patel, M.P., Rajani, D.P., Patel, R.G., 2011. *Eur. J. Med. Chem.* 46, 4192–4200.
- Nadagouda, M.N., Speth, T.F., Varma, R.S., 2011. *Acc. Chem. Res.* 44, 469–478.
- Nakhjavani, M., Mohsen Sarafraz, M., Nikkhal, V., Shoja, S., Sarafraz, M., 2017. *Heat Mass Transf.* 53, 3201–3209.
- Oves, M., Aslam, M., Rauf, M.A., Qayyum, S., Qari, H.A., Khan, M.S., et al., 2018. *Mater. Sci. Eng., C* 89, 429–443.
- Patil, M.P., Kim, G.-D., 2017. *Appl. Microbiol. Biotechnol.* 101, 79.
- Philip, D., Unni, C., Aromal, S.A., Vidhu, V.K., 2011. *Spectrochim. Acta Part A Mol. Biomol. Spectrosc.* 78 (2), 899–904.
- Pradhan, K., Paul, S., Das, A.R., 2014. *Catal. Sci. Technol.* 4, 822–831.
- Prashanth, M.I., Shivamaruthi, B.S., Chaiyasut, C., Tencomnao, T., 2019. *Nutrients* 11, 474.
- Rai, M., Ingle, A., 2012. *Appl. Microbiol. Biotechnol.* 94, 287–293.
- Rautela, A., Rani, J., Debnath, M., 2019. *J. Anal. Sci. Technol.* 10 (5), 1–10.
- Santhoshkumar, T., Rahuman, A.A., Rajakumar, G., Marimuthu, S., Bagavan, A., Jayaseelan, C., Zahir, A.A., Elango, G., Kamaraj, C., 2011. *Parasitol. Res.* 108 (3), 693–702.
- Saundane, A.R., Vijaykumar, K., Vaijinath, A.V., 2013. *Bioorg. Med. Chem. Lett.* 23, 1978–1984.
- Shahriari, M., Sedigh, M.A., Mahdavian, Y., Mahdigholizad, S., Pirhayati, M., Karmakar, B., Veisi, H., 2021. *Int. J. Biol. Macromol.* 172, 55–61.
- Sharma, V.K., Yngard, R.A., Lin, Y., 2009. *Adv. Colloid. Interfac.* 145, 83–96.
- Shivashankar, K., Kulkarni, M.V., Shastri, L.A., Rasal, V.P., Rajendra, S.V., 2006. *Phosphorus, Sulfur Silicon Relat. Elem.* 181, 2187–2200.
- Shivashankar, K., Shastri, L.A., Kulkarni, M.V., Rasal, V.P., Rajendra, S.V., 2007. *Phosphorus, Sulfur Silicon Relat. Elem.* 183, 56–68.
- Siddiqi, K.S., Husen, A., Rao, R.A.K., 2018. *J. Nanobiotechnol.* 16 (14), 1–28.
- Singh, S., Bharti, A., Meena, V.K., 2015. *J. Mater. Sci.: Mater. Electron.* 26, 3638–3648.
- Singh, M.S., Nandi, G.C., Samai, S., 2012. *Green Chem.* 14, 447–455.
- Suman, T.Y., Radhika Rajasree, S.R., Kanchana, A., Elizabeth, S.B., 2013. *Colloids Surf B. Biointerfaces* 106, 74–78.
- Vala, N.D., Jardosh, H.H., Patel, M.P., 2016. *Chin. Chem. Lett.* 27, 168–172.
- Valeri, N., 2019. *Cancer Res.* 79, 1041–1043.
- Vankar, P.S., Shukla, D., 2012. *Appl. Nanosci.* 2, 163–168.
- Vartooni, A.R., Nasrollahzadeh, M., Alizadeh, M., 2016. *J. Colloid Interface Sci.* 470, 268–275.
- Veisi, H., Azizi, S., Mohammadi, P., 2018. *J. Clean. Prod.* 170, 1536–1543.
- Veisi, H., Kazemi, S., Mohammadi, P., Safarimehr, P., Hemmati, S., 2019. *Polyhedron* 157, 232–240.
- Venkatesham, A., Rao, R.S., Nagaiah, K., Yadav, J.S., Jones, G.R., Basha, S.J., Sridhar, B., Addlagatta, A., 2012. *Med. Chem. Comm.* 3, 652–658.
- Wang, H.-J., Lu, J., Zhang, Z.-H., 2010. *Monatsh. Chem.* 141, 1107–1112.
- Wang, R., Yang, Z., Zhang, J., Mu, J., Zhou, X., Zhao, X., 2019. *Antioxidants* 8 (3), 64.
- Zhang, R.-R., Liu, J., Zhang, Y., Hou, M.-Q., Zhang, M.-Z., Zhou, F., Zhang, W.-H., 2016. *Eur. J. Med. Chem.* 116, 76–83.
- Zhang, X.F., Liu, Z.G., Shen, Gurunathan, W.S., 2016. *Int. J. Mol. Sci.* 17, E1534.
- Zomorodian, K., Veisi, H., Mousavi, S.M., Ataabadi, M.S., Yazdanpanah, S., Bagheri, J., Parvizi Mehr, A., Hemmati, S., Veisi, H., 2018. *Int. J. Nanomed.* 13, 3965.